Electronic Supplementary Information

TGA of MNPs was carried out in Fig. S2. The results of weight loss for MNPs and Hoechst MNPs were 10% and 14%, respectively. Hoechst attached on the MNP account for the extra 4% weight loss as compared to that of MNPs. This fact supports that Hoechst was successfully conjugated on the MNPs. Superparamagnetism is especially important in applications such as targeting delivery since the elimination of the magnetic force for aggregation. Moreover, superparamagnetic nanoparticles provide a strong response to an external magnetic field (Fig. S3). Two typical magnetization curves for magnetic nanoparticles showed the characteristic sigmoidal curve under an external field. The saturation magnetization values of MNPs and Hoechst MNPs were 20 and 40 emu/g Fe, respectively. The modified iron oxides are superparamagnetic and show negligible hysteresis. A typical TEM photograph of MNPs is shown in Fig. S4. The morphology of two kinds of MNPs can be observed. The size distribution of both MNPs was uniform with the average size of 8.25±0.96 nm. The size of Hoechst MNPs was around 14.60±2.43 nm. Additionally, 6 nm increase in MNPs' size was observed after Hoechst modification. Effect of pH values on surface potential of MNPs was summarized in Fig. S4. The surface charges (zeta potentials) on the surfaces of the nanoparticles were also studied by using the Zetasizer (Malvern). Solutions with different pH values were used to study the surface charge on the surfaces of nanoparticles. These magnetic nanoparticles could be well suspended in the various pH solutions without precipitation. Fluorescence emission spectra of various MNPs synthesized at different pH values and Hoechst dye are shown in Fig. S5. The results indicated that Hoechst MNPs synthesized at pH 11 had the strongest fluorescence when in contact with DNA. The fluorescence photos of Hoechst MNPs and DNA mixture (Fig. S6) also supported this conclusion.

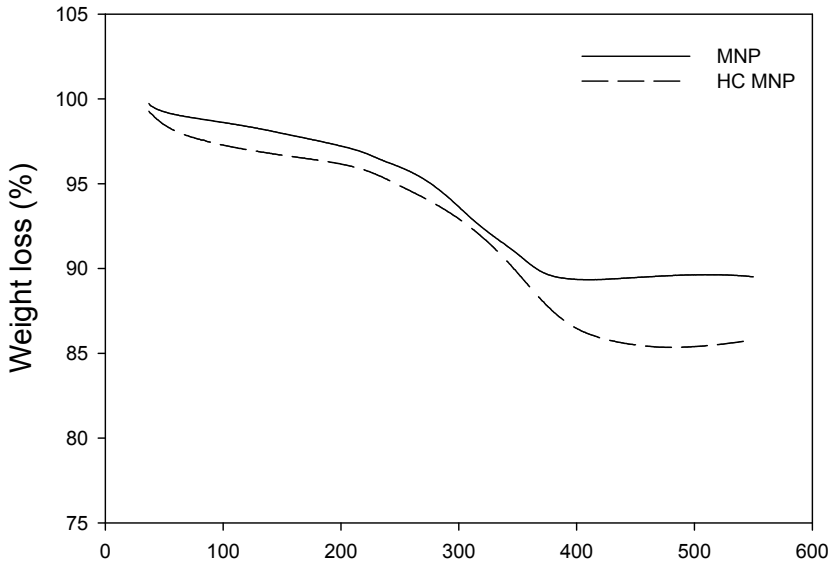

Fig. S1. TGA profile of MNPs and Hoechst MNPs.

Thermogravimetric analysis (TGA) was conducted using a Perkin-Elmer TGA 7 at a constant heating rate of 10 °C/min from room temperature to 550 °C in a nitrogen environment.

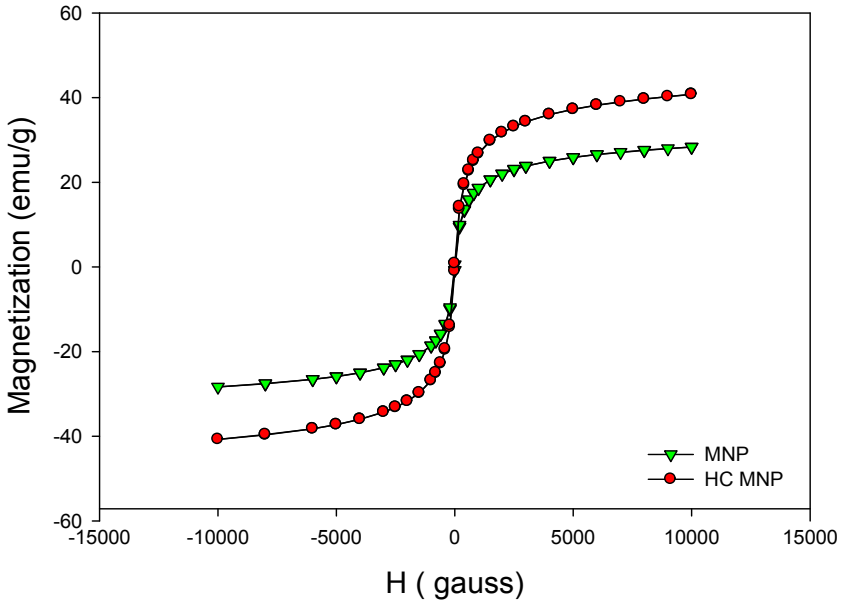

Fig. S2. Magnetization curve as a function of magnetic field for MNPs and Hoechst MNPs at a temperature of 25 °C.

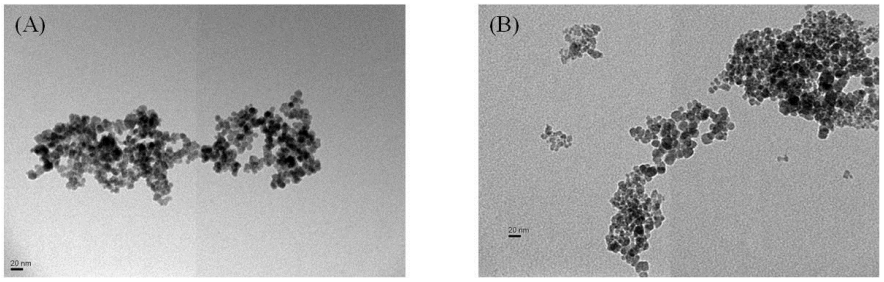

Fig. S3. TEM microstructure for MNPs (A) and Hoechst MNPs (B). The scale bar is 20 nm. The magnification is 300K.

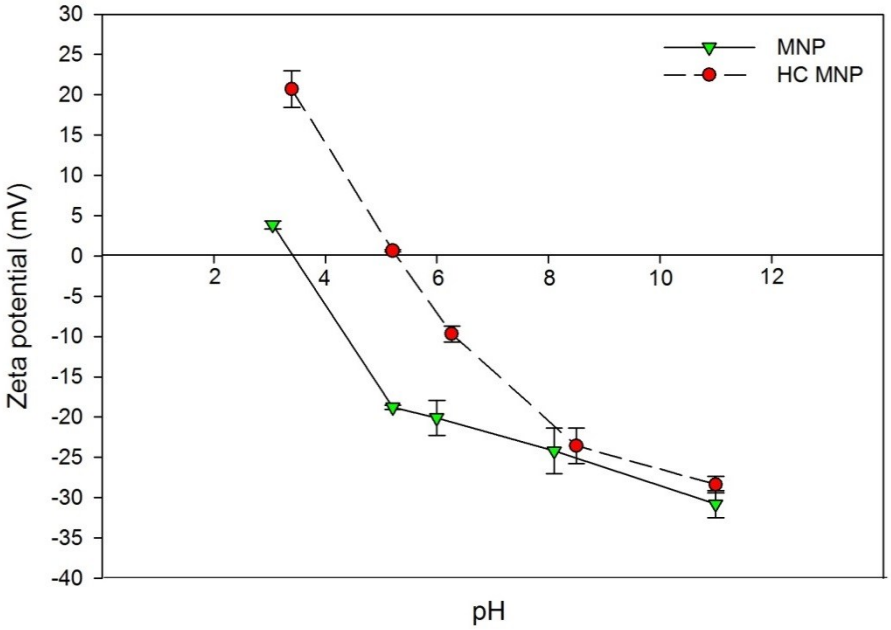

Fig. S4. Zeta potential of MNPs and Hoechst MNPs at different pH values. The data are the average of triplicate experiments.

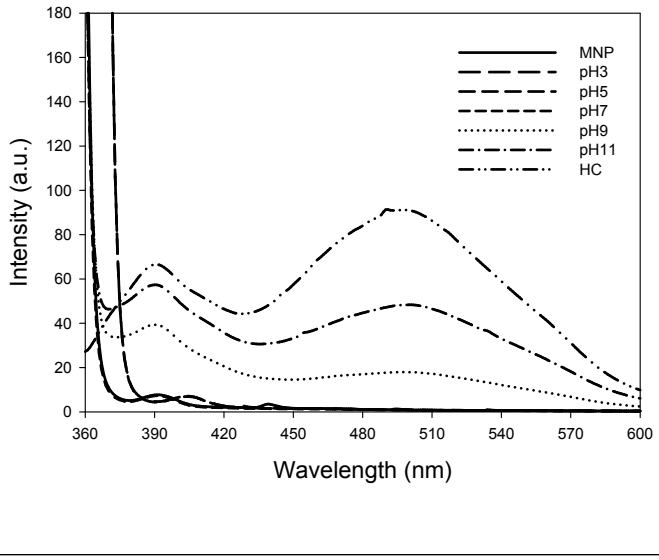

(A) Absence of plasmid DNA

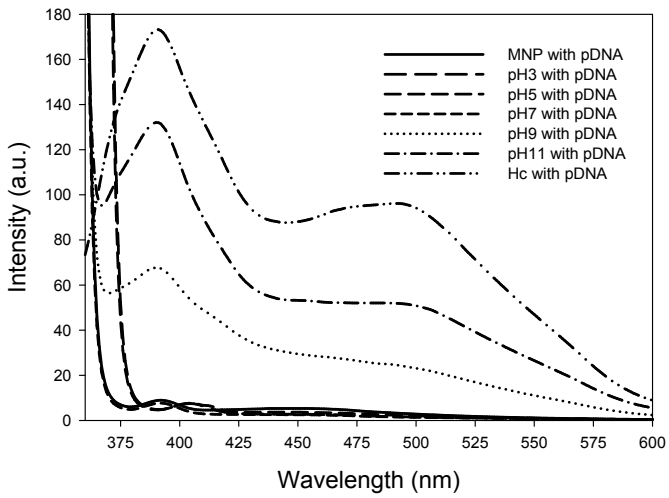

(B) Presence of plasmid DNA

Fig. S5. Fluorescence emission spectra of bare MNPs, various Hoechst MNPs synthesized at different pH values and Hoechst dye in the absence (A) or presence (B) of plasmid DNA. The Hoechst MNPs were synthesized at different pH conditions.

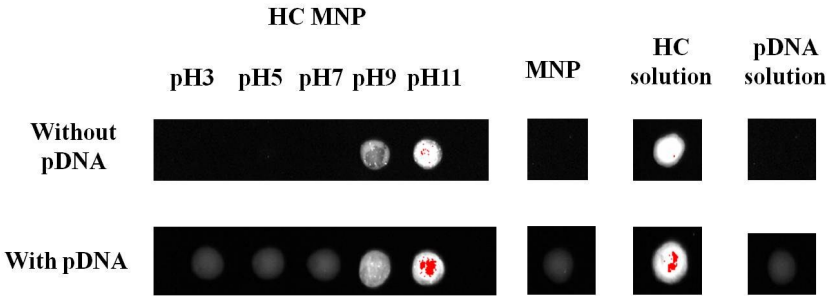

Fig. S6. Fluorescent photos of bare MNPs, Hoechst MNPs synthesized at different pH conditions and free Hoechst in the absence (A) or presence (B) of plasmid DNA. Plasmid DNA (556 ng/μL, 10 μL) was mixed with Hoechst MNPs (10 μL) and Hoechst under a UV lamp (302 nm). The stock concentrations of Hoechst and Hoechst-MNPs were 1700 μg/mL and 1000 μg/mL, respectively.

The Fourier transform infrared spectra of the original MNPs (containing carboxyl groups) and Hoechst-modified magnetic particles are presented in Fig. (S7A and B). The Hoechst MNPs showed distinct peaks at 1631 cm-1, and these have been reportedly attributed to the stretching of the amide I band[41]. Based on the

above results, it was confirmed that HC MNPs was successfully formed.

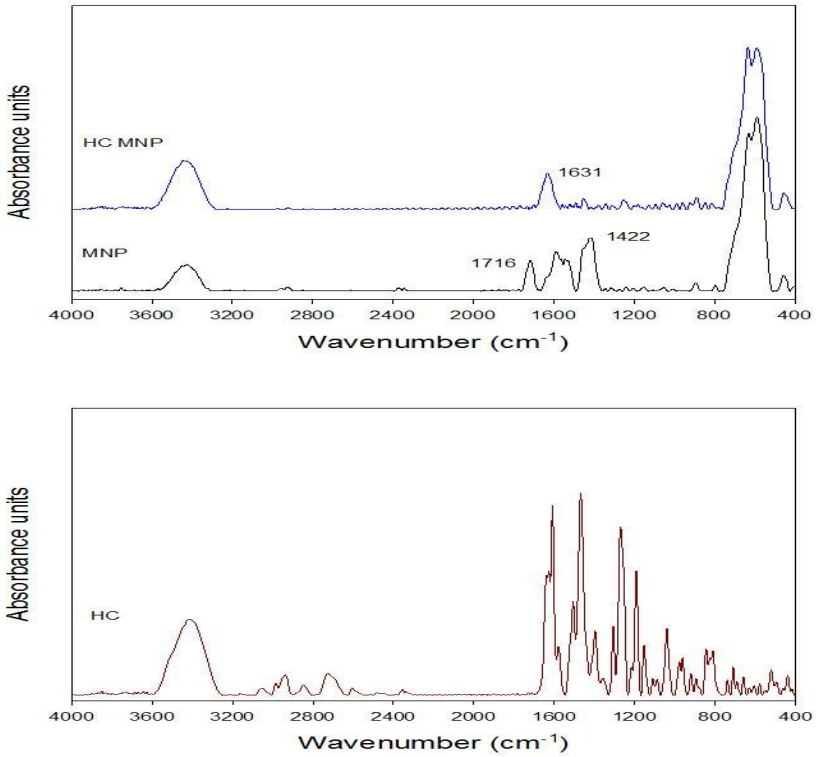

Fig. S7. FTIR spectra of HC MNPs, MNPs (A) and HC (B).

Fluorescent photos of ssDNA and pDNA adsorption by HC MNPs are shown in Fig. S8. Different concentrations of DNA in presence of 0.5M $CaCl_2$ are incubated for 30 minutes at RT and after magnetic separations, the DNA adsorbed by HC MNPs and the remaining DNA in the supernatant were imaged under a UV lamp (302 nm), Bio-Rad imaging system. The remaining DNA in the supernatant was much less than the separated DNA. From the DNA intensity in the images, we found that less than 20~30% of unbound DNA remained in the supernatant. These results roughly indicated that the high capacity of HC MNPs for pDNA and ssDNA.

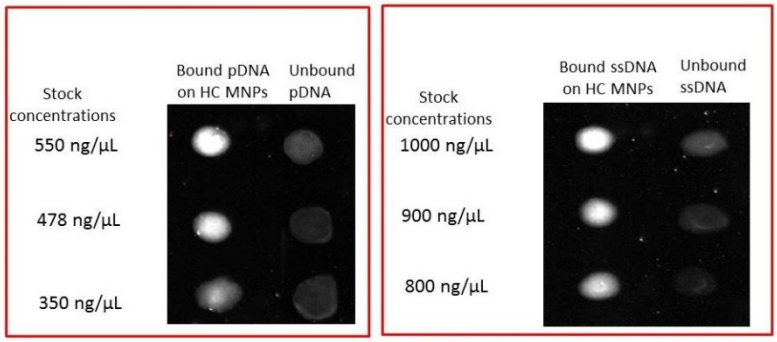

Fig. S8. Images of the unbound DNA after the adsorption and the adsorbed DNA using the Bio-Rad imaging system. Plasmid DNA (350-550 ng/µL, 10 µL) or ssDNA (800-1000 ng/µL, 10 µL) was incubated with Hoechst MNPs (10 µL) and 0.5M $CaCl_2$ for 30 minutes at RT. After magnetic separation, HC MNPs with DNA and the remaining DNA in the supernatant were imaged under a UV lamp (302 nm), Bio-Rad imaging system.

The hydrodynamic diameters of MNPs and HC MNPs in aqueous solution were determined by dynamic light scattering (DLS) analysis (Table S1). The results indicated that the dispersion of MNPs and HC MNPs in water exhibits poorly stabilized and aggregated. The diameter of MNPs and HC MNPs increased in water, while in PBS and cell culture medium (DMEM) the aggregation properties reduced and diameter decreased. The observed hydrodynamic diameter of HC MNPs in cell culture medium is 68.7 nm. The possible stabilizing agent in medium is serum albumin, which carries a negative charge at physiologic pH and therefore may stabilize the particles by imparting a net surface charge[42]. Compared to the size observed in TEM, the corresponding hydrodynamic diameters of MNPs and HC MNPs are much larger. Table S1. However, the size ranges from 10-100 nm of the nanoparticles can be efficiently endocytosis by various types of cells [43].

Table S1. Hydrodynamic size distribution of MNPs and HC MNPs dispersed in DDW, PBS, and Medium (DMEM).

MNPs	Medium (DMEM)	PBS	DDW
MNPs	49.6 nm	110 nm	135.7 nm
Hoechst MNPs	68.7 nm	118 nm	143.6 nm